

INFLUENCE OF PROCESSING CONDITIONS ON CRYSTAL STRUCTURE OF $\text{Bi}_6\text{Fe}_2\text{Ti}_3\text{O}_{18}$ CERAMICS

Aim of the present research was to apply a solid state reaction route to fabricate Aurivillius-type ceramics described with the formula $\text{Bi}_6\text{Fe}_2\text{Ti}_3\text{O}_{18}$ (BFTO) and reveal the influence of processing conditions on its crystal structure. Pressureless sintering in ambient air was employed and the sintering temperatures were 850 and 1080 °C. It was found that the fabricated BFTO ceramics were multiphase ones. They consisted of two $\text{Bi}_{m+1}\text{Fe}_{m-3}\text{Ti}_3\text{O}_{3m+3}$ phases, namely the phase with $m=5$ (i.e. the stoichiometric phase) and $m=4$ (i.e. the phase with a reduced number of layers in the slab). Detailed X-ray diffraction patterns analysis showed that both phases adopted the same orthorhombic structure described with $Fmm2$ (42) space group. The ratio of weight fractions of the constituent phases ($m=5$): ($m=4$) was ~30:70.

1. Introduction

One of the very promising approaches to create novel materials is to combine in one material different physical properties to achieve rich functionality. It is commonly known that Aurivillius phases of $\text{Bi}_4\text{Ti}_3\text{O}_{12}$ - BiFeO_3 (BFTO) system, combine ferroelectric, semiconducting and ferromagnetic properties and are potentially attractive for producing high-performance ceramics for information processing and information storage applications [1, 2]. Among the different ferromagnetic compounds of BFTO system $\text{Bi}_6\text{Fe}_2\text{Ti}_3\text{O}_{18}$ was found to be interesting because of the high dielectric transition temperature ($T=805^\circ\text{C}$) and quadratic magnetoelectric nature [3].

It is worth noting that $\text{Bi}_6\text{Fe}_2\text{Ti}_3\text{O}_{18}$ compound has a layered perovskite-like structure described with the general formula $\text{Bi}_{m+1}\text{Fe}_{m-3}\text{Ti}_3\text{O}_{3m+3}$, ($m=5$). Perovskite-like layered structure consists of the fluorite-like bismuth-oxygen layers of composition $\{(\text{Bi}_2\text{O}_2)^{2+}\}_\infty$ which alternate with (001) perovskite-like slabs of composition $\{(\text{Bi}_{m+1}\text{Fe}_{m-3}\text{Ti}_3\text{O}_{3m+1})^{2-}\}_\infty$. The values of m indicates the number of perovskite-like layers per slab and may take integer or fractional values [4, 5].

Although several researches on $\text{Bi}_6\text{Fe}_2\text{Ti}_3\text{O}_{18}$ ceramics have already been performed either by us [e.g. 6, 7] or other scientific groups [e.g. 8, 9, 10,] however low temperature dielectric behavior of BFTO was not studied yet. Therefore the present research was focused on fabrication of and study of dielectric response of Aurivillius structure multiferroic ceramics.

2. Experimental

The mixed oxide method was employed for the ceramics fabrication. Simple oxide powders Bi_2O_3 , TiO_2 and Fe_2O_3 were

used for stoichiometric mixture preparation. Parameters of the thermal treatment were determined by simultaneous thermal analysis (DTA/TG/DTG). The measurements were obtained with Netzsch STA409 thermal analyzer. After calcinations process ($T_{calc}=720^\circ\text{C}$) the pellets were formed and pressed into disks with the diameter of 10mm and 1mm thickness. Pressureless sintering was used for final densification of ceramic samples. Sintering temperatures were $T_s=850^\circ\text{C}$, $T_s=1080^\circ\text{C}$, whereas the soaking time was $t_s=2\text{h}$ in both experiment sets.

The crystalline structure of the sintered samples were examined by X-ray diffraction at room temperature (X'Pert – Pro diffractometer, $\theta - 2\theta$ mode). It should be mentioned that for the sample sintered at $T_s=850^\circ\text{C}$ the $\text{CuK}\alpha$ radiation was used ($\lambda\alpha_1=1.54060 \text{ \AA}$; $\lambda\alpha_2=1.54443 \text{ \AA}$; ratio $\alpha_{21}=0.5$; data angle range $2\theta= 8.0042 - 89.9962^\circ$; detector scan step size $\Delta 2\theta=0.008^\circ$; scan type continuous; scan step time $t=99.7\text{s}$), whereas for BFTO ceramics sintered at $T_s=1080^\circ\text{C}$ the $\text{CoK}\alpha$ radiation was utilized ($\lambda\alpha_1=1.78901 \text{ \AA}$; $\lambda\alpha_2=1.7929 \text{ \AA}$; ratio $\alpha_{21}=0.5$; data angle range $2\theta=10.0042- 104.9962^\circ$; detector scan step size $\Delta 2\theta=0.008^\circ$; scan type continuous; scan step time $t=302.9\text{s}$).

Analysis of the X-ray diffraction patterns was carried out using X'pert HighScore Plus software (PANalytical B.V), Match! (Crystal Impact, Inc.) computer program [11]. The latest available COD [11], ICSD [12] and ICDD [13] databases were utilized.

3. Results and discussion

Thermal analysis. Simultaneous thermal analysis (STA), in which both thermal analysis (DTA) and mass change effects

* UNIVERSITY OF SILESIA, INSTITUTE OF TECHNOLOGY AND MECHATRONICS, 12 ŻYTNIA STR, 41-200 SOSNOWIEC, POLAND

** PEDAGOGICAL UNIVERSITY, INSTITUTE OF ENGINEERING, 2 PODCHORAŻYCH STR., 30-084 KRAKÓW, POLAND

*** PEDAGOGICAL UNIVERSITY, INSTITUTE OF PHYSICS, 2 PODCHORAŻYCH STR., 30-084 KRAKÓW, POLAND

Corresponding author: agata.lisinska-czekaj@us.edu.pl

(TG) are measured concurrently on the same sample was used to investigate synthesis effects in the stoichiometric mixture of powders. Results of STA of the stoichiometric mixture of the oxides forming $\text{Bi}_6\text{Fe}_2\text{Ti}_3\text{O}_{18}$ compound are given in Fig. 1.

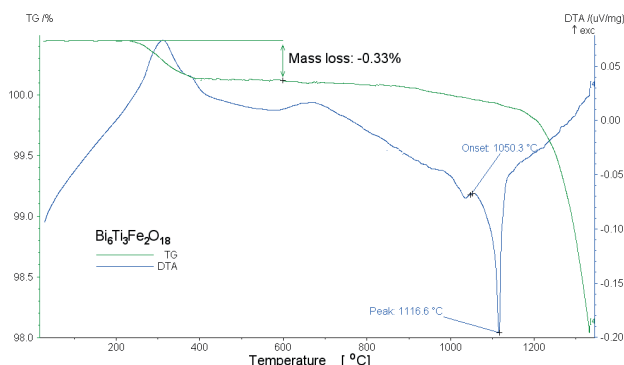


Fig. 1. Results of thermal analysis of stoichiometric mixture of oxides forming $\text{Bi}_6\text{Fe}_2\text{Ti}_3\text{O}_{18}$

One can see on a thermogravimetric (TG) curve shown in Fig. 1 that the total mass loss during the heat treatment of the stoichiometric mixture of Bi_2O_3 , Fe_2O_3 , and TiO_2 oxides at $T=600^\circ\text{C}$ reaches a value of about $\Delta m = -0.33\%$. The DTA study revealed thermal effects manifested upon heating the samples. One can see a relatively broad, exothermic peak that appears in the differential thermogram at $T \approx 300^\circ\text{C}$. It corresponds to the mass change effects present in the sample.

The experimental data on kinetics of the formation of layered perovskitelike compounds in the BFTO system have shown that detectable amounts of Aurivillius phases appear at 600°C [14]. This temperature is close to the melting point of the $\gamma\text{-Bi}_2\text{O}_3$ -based surface phase, ($T_m^{\text{surf}} \approx 550\text{--}630^\circ\text{C}$) at which a sharp increase in the rate of mass transfer activates chemical reactions limited by the rate of transport processes. At still higher temperatures, the percentage of layered perovskite-like compounds rises systematically and reaches a maximum at the melting point of the $\gamma\text{-Bi}_2\text{O}_3$ -based bulk phase T_m^{surf} . Therefore

the broad exothermic effect at the temperature range $\Delta T \approx 650\text{--}700^\circ\text{C}$ (Fig. 1) can be tentatively attributed to formation of BFTO phases.

The weak endothermic peak at about $T \approx 1036^\circ\text{C}$, one can ascribed to the phase transformations, namely a peritectic decomposition into compounds of the same homologous series with a smaller number of perovskite – like layers in their structure [2], whereas the strong endothermic peak at $T \approx 1117^\circ\text{C}$ – to liquidus temperature [2, 15].

4. X-ray diffraction phase and structural analysis

Results of the qualitative XRD phase analysis for BFTO ceramics produced by solid-phase chemical reactions and sintered at temperatures $T=850$ and 1080°C , is given in Fig. 2, Tab. 1 and Fig. 3, Tab. 2, respectively.

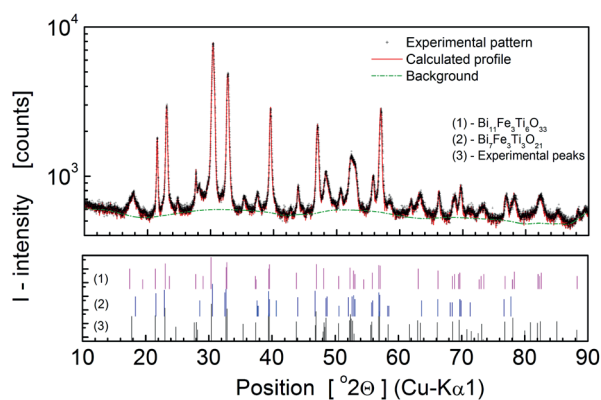


Fig. 2. X-ray diffraction matching parameters for $\text{Bi}_6\text{Fe}_2\text{Ti}_3\text{O}_{18}$ ceramics fabricated via solid state reaction route and pressureless sintering at $T=850^\circ\text{C}$; (bottom plot – peak positions of the experimental pattern and the main reference phases)

One can see that the results indicated that the forming Aurivillius phases had an imperfect structure, which may not correspond to the stoichiometric composition owing to

TABLE 1

Matched phases for BFTO powder after sintering at $T=850^\circ\text{C}$

Weight fraction, %	Formula/Space group/Crystal system	Unit cell parameters	Number of peaks		FoM
			total	matched	
50.8	$\text{Bi}_{11}\text{Fe}_3\text{Ti}_6\text{O}_{33}$ / $Bm2m$ / orthorhombic	$a = 5.4730 \text{ \AA}$ $b = 45.4200 \text{ \AA}$ $c = 5.4500 \text{ \AA}$	total	42	0.8565
			in range	41	
			matched	35	
43.2	$\text{Bi}_7\text{Fe}_3\text{Ti}_3\text{O}_{21}$ / $F2mm$ / orthorhombic	$a = 5.4950 \text{ \AA}$ $b = 57.5810 \text{ \AA}$ $c = 5.4710 \text{ \AA}$	total	39	0.8036
			in range	39	
			matched	32	
2.5	$\text{Bi}_{25}\text{FeO}_{40}$ / $I23$ / cubic	$a = 10.1789 \text{ \AA}$	total	41	0.7309
			in range	40	
			matched	19	
1.9	$\text{Bi}_5\text{FeTi}_3\text{O}_{15}$ / $Fmm2$ / orthorhombic	$a = 5.4318 \text{ \AA}$ $b = 41.1490 \text{ \AA}$ $c = 5.4691 \text{ \AA}$	total	171	0.8328
			in range	162	
			matched	71	
1.6	$\text{Bi}_{12}\text{TiO}_{20}$ / $I23$ / cubic	$a = 10.1880 \text{ \AA}$	total	41	0.7137
			in range	40	
			matched	20	

a reduced number of layers ($m=3, m=4, m=4.5$) in the slab or disordered stacking of the layers.

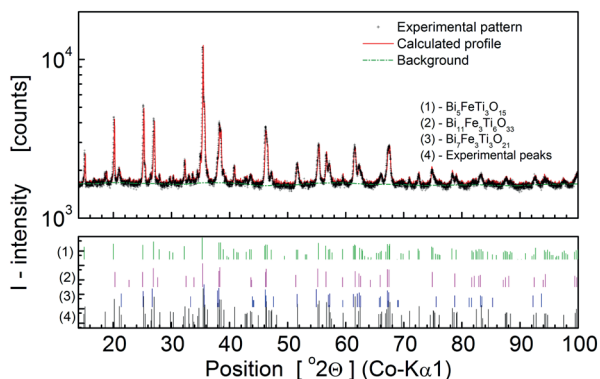


Fig. 3. X-ray diffraction matching parameters for $\text{Bi}_6\text{Fe}_2\text{Ti}_3\text{O}_{18}$ ceramics fabricated via solid state reaction route and pressureless sintering at $T=1080^\circ\text{C}$; (bottom plot – peak positions of the experimental pattern and the main reference phases)

According to the suggested scheme for the formation of Aurivillius phases in the $\text{Bi}_2\text{O}_3\text{--TiO}_2\text{--Fe}_2\text{O}_3$ system the formation of $\text{Bi}_{m+1}\text{Fe}_{m-3}\text{Ti}_3\text{O}_{3m+3}$ compound is considered as a multistage process [16]. At early stages compounds with smaller numbers of perovskite-like layers in the structure and BiFeO_3 are formed. At the next stage, perovskite-like BiFeO_3 is incorporated into a perovskite-like layer of Aurivillius phases to increase the thickness of this layer until an Aurivillius phase of a given composition is formed. In the course of further heat treatment, the number of perovskite layers in the slab approaches that corresponding to the stoichiometric composition, and the proportion of intermediate synthesis products drops.

In his connection it should be pointed out that both $\text{Bi}_{12}\text{TiO}_{20}$ and $\text{Bi}_{25}\text{FeO}_{40}$ are intermediate synthesis Bi_2O_3 -reach products that appear around $T=500^\circ\text{C}$ as the $\alpha\text{-Bi}_2\text{O}_3$ reacted with small amounts of TiO_2 and Fe_2O_3 . These compounds are extremely difficult to distinguish by XRD, since both are isostructural and have a structure closely similar to that of the

metastable phase $\gamma\text{-Bi}_2\text{O}_3$ (see Tab. 1) [14]. The amount of these phases in the final ceramic product is quite small – on the level of the resolution of the method ($\pm 3\%$) and can be neglected in the further analysis.

With an increase in the sintering temperature, amount of the intermediate Bi_2O_3 -reach compounds decreased and formation of Aurivillius phases took place. One can see in Fig. 3 and Tab. 2 that phases with a small number of layers m in the slab have been formed, namely $m=3$ - $\text{Bi}_4\text{Ti}_3\text{O}_{12}$, $m=4$ - $\text{Bi}_5\text{FeTi}_3\text{O}_{15}$ and $m=4.5$ - $\text{Bi}_{11}\text{Fe}_3\text{Ti}_6\text{O}_{33}$.

On the base of the phase analysis one can conclude that $\text{Bi}_{m+1}\text{Fe}_{m-3}\text{Ti}_3\text{O}_{3m+3}$ compounds are difficult to produce because these compounds are formed in several stages and their thermal stability is low.

Detailed structural analysis, together with refinement of the elementary cell parameters (according to the Rietveld method [e.g. 17]) was performed for X-ray diffraction patterns of $\text{Bi}_6\text{Fe}_2\text{Ti}_3\text{O}_{18}$ ceramics fabricated via solid state reaction route and pressureless sintering at $T=850$ and 1080°C . Visual results of the performed analysis are shown in Fig. 4 and Fig. 5. Global parameters of the structural analysis are shown in Tab. 3, whereas structure parameters of the constituent phases are given in Tab. 4.

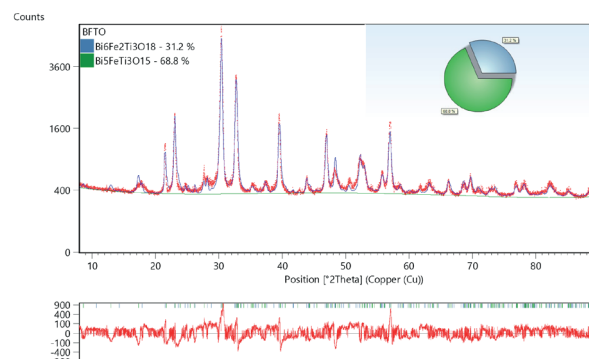


Fig. 4. X-ray diffraction pattern after refinement of the elementary cell parameters for BFTO ceramics sintered at $T=850^\circ\text{C}$ in assumption of the multiphase sample; bottom plot shows the difference between the experimental (dots) and refined (solid line) diffraction patterns

Matched phases for BFTO powder after sintering at $T=1080^\circ\text{C}$

Weight fraction, %	Formula/Space group/Crystal system	Unit cell parameters	Number of peaks		FoM
			total	matched	
49.6	$\text{Bi}_{11}\text{Fe}_3\text{Ti}_6\text{O}_{33}$ / $Bm2m$ / orthorhombic	$a = 5.4730 \text{ \AA}$ $b = 45.4200 \text{ \AA}$ $c = 5.4500 \text{ \AA}$	total	42	0.8206
			in range	41	
			matched	33	
30.8	$\text{Bi}_7\text{Fe}_3\text{Ti}_3\text{O}_{21}$ / $F2mm$ / orthorhombic	$a = 5.4950 \text{ \AA}$ $b = 57.5810 \text{ \AA}$ $c = 5.4710 \text{ \AA}$	total	39	0.7677
			in range	39	
			matched	29	
17.2	$\text{Bi}_5\text{FeTi}_3\text{O}_{15}$ / $Fmm2$ / orthorhombic	$a = 5.4318 \text{ \AA}$ $b = 41.1490 \text{ \AA}$ $c = 5.4691 \text{ \AA}$	total	144	0.8732
			in range	131	
			matched	88	
1.4	$\text{Bi}_{25}\text{FeO}_{40}$ / $I23$ / cubic	$a = 10.1789 \text{ \AA}$	total	41	0.6931
			in range	38	
			matched	21	
1.0	$\text{Bi}_4\text{Ti}_3\text{O}_{12}$ / $B2cb$ / orthorhombic	$a = 5.4451 \text{ \AA}$ $b = 5.4101 \text{ \AA}$ $c = 32.8565 \text{ \AA}$	total	286	0.7170
			in range	209	
			matched	69	

TABLE 2

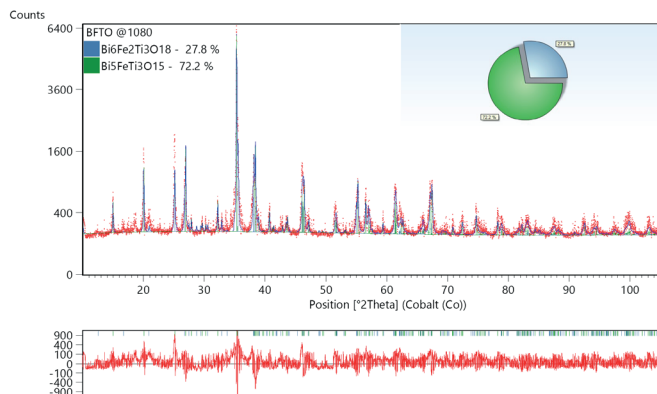


Fig. 5. X-ray diffraction pattern after refinement of the elementary cell parameters for BFTO ceramics sintered at $T=1080\text{ }^{\circ}\text{C}$ in assumption of the multiphase sample; bottom plot shows the difference between the experimental (dots) and refined (solid line) diffraction patterns.

One can see from Tab. 3 that Rietveld refinement of the crystal structure of fabricated BFTO ceramics was performed with good quality so the data obtained are correct and reasonable. It was found that the samples were multiphase ones. They consisted of two BFTO Aurivillius phases with consecutive, integer number of layers m in the slab, namely $m=4$ and $m=5$. The dominant phase in the BFTO ceramics was the one with $m=4$. The weight fraction of a BFTO phase with a reduced number of layers (m) in the slab increased from 69% to 72% with an increase in the sintering temperature.

It should be noted, however, that both phases were described with the same orthorhombic symmetry, the same space group ($Fmm2$) and it is likely that they exhibited the same axis setting. Taking into consideration the above mentioned and the fact that ratio of weight fractions of the constituent phases ($m=5$):($m=4$) in fabricated BFTO ceramics is almost independent on sintering temperature one can postulate that the resultant phase can be an Aurivillius mixed phase [e.g. 18, 19] described with a fractional number $m\approx(4.3\pm 0.02)$. However, The Authors realize that the above mentioned hypothesis needs further investigations on synthesis of BFTO ceramics.

5. Conclusions

Single-phase samples of $\text{Bi}_6\text{Fe}_2\text{Ti}_3\text{O}_{18}$ compounds are difficult to produce by solid-phase chemical reactions because these compounds are formed in several stages and their thermal stability is low. Results of the XRD analysis indicated that the forming Aurivillius phases had an imperfect structure. They corresponded to the mixture of $\text{B}_{m+1}\text{Fe}_{m-3}\text{Ti}_3\text{O}_{3m+3}$ compositions with both stoichiometric ($m=5$) and reduced ($m=4$) number of perovskite-like layers (m) in the slab. The ratio of weight fractions of the constituent phases ($m=5$): ($m=4$) was found to be $\sim 30:70$.

It was found that the influence of sintering temperature, within the chosen range, on crystal structure and phase composition of BFTO ceramics was rather minor. However, a small increase in the amount of BFTO phase with $m=4$ was observed.

TABLE 3

Global parameters of the Rietveld analysis for X-ray diffraction patterns of BFTO ceramic,

Parameter	Value	
	BFTO @ $T=850\text{ }^{\circ}\text{C}$	BFTO @ $T=1080\text{ }^{\circ}\text{C}$
Profile function:	Pseudo Voigt	Pseudo Voigt
Background:	Polynomial	Polynomial
R (expected)/ %:	5.07159	8.17205
R (profile)/ %:	7.01839	14.12068
R (weighted profile)/ %:	8.75605	13.59406
GOF:	2.98076	2.76718

TABLE 4

Structure parameters of the constituent phase,

Relevant parameters	BFTO @ $T=850\text{ }^{\circ}\text{C}$		BFTO @ $T=1080\text{ }^{\circ}\text{C}$	
	$\text{O}_{72}\text{Fe}_8\text{Ti}_{12}\text{Bi}_{24}$	$\text{O}_{60}\text{Fe}_4\text{Ti}_{12}\text{Bi}_{20}$	$\text{O}_{72}\text{Fe}_8\text{Ti}_{12}\text{Bi}_{24}$	$\text{O}_{60}\text{Fe}_4\text{Ti}_{12}\text{Bi}_{20}$
Formula sum	$\text{O}_{72}\text{Fe}_8\text{Ti}_{12}\text{Bi}_{24}$	$\text{O}_{60}\text{Fe}_4\text{Ti}_{12}\text{Bi}_{20}$	$\text{O}_{72}\text{Fe}_8\text{Ti}_{12}\text{Bi}_{24}$	$\text{O}_{60}\text{Fe}_4\text{Ti}_{12}\text{Bi}_{20}$
Formula mass/ g/mol	7189.062	5937.76	7189.062	5937.76
Density calculated	8.0683	8.0901	8.0766	8.0554
Weight fraction/ %:	31(1)	69(1)	28(1)	72(1)
Space group (No.):	F m m 2 (42)	F m m 2 (42)	F m m 2 (42)	F m m 2 (42)
Lattice parameters:				
a/ Å	5.467(9)	5.459(2)	5.4863(7)	5.4398(3)
b/ Å:	49.485(5)	40.851(6)	49.263(6)	41.135(3)
c/ Å:	5.468(9)	5.465(1)	5.4680(8)	5.4693(4)
V/ 10^6 pm^3	1479.37	1218.579	1477.853	1223.839
R (Bragg)/ %:	6.21572	6.22126	12.50063	11.22527

Acknowledgements

The present research was supported by University of Silesia in Katowice, Poland from the funds for science – research potential (NO 1S-0800-001-1-05-01).

REFERENCES

- [1] M. Krzhizhanovskaya, S. Filatov, V. Gusarov, P. Paufler, R. Bubnova, M. Morozov, D. Meyer, *Anorg. Allg. Chem.* **631**, 1603 – 1608 (2005).
- [2] N.A. Lomanova, M.I. Morozov, V.L. Ugolkov, V.V.Gusarov, *Inorg. Mater.* **42**, 189 – 195 (2006).
- [3] E. Jartych, M. Mazurek, A. Lisińska-Czekaj, D. Czekaj, *Journal of Magnetism and Magnetic Materials* **322**, 51–55 (2010).
- [4] A. Lisińska-Czekaj, *Wielofunkcyjne materiały ceramiczne na osnowie tytanianu bizmutu*, Wydawnictwo Gnome, Uniwersytet Śląski, Katowice 2012.
- [5] A. Lisińska-Czekaj, D. Czekaj, *Ferroelektryki o warstwowej strukturze perowskitopodobnej BWPT*. W: Z.Surowiak (Red.) *Elektroceramika ferroelektryczna*, Wydawnictwo Uniwersytetu Śląskiego, Katowice (2004).
- [6] A. Lisińska-Czekaj, *Materials Science Forum* **730-732**, 100-104 (2013).
- [7] A. Lisińska-Czekaj, D. Czekaj, *Materials Science Forum* **730-732**, 76-81 (2013).
- [8] K. Srinivas, P. Sarah, S.V. Suryanarayana, *Bulletin of Materials Science* **26**, (2), 247–253 (2003).
- [9] D. Zientara, M. Bućko, J. Polnar, *Advances in Science and Technology* **67**, 164-169 (2010).
- [10] M. Bućko, J. Polnar, J. Przewoźnik, J. Żukrowski, Cz. Kapusta, *Advances in Science and Technology* **67** 170-175 (2010).
- [11] <http://www.crystalimpact.com/match>
- [12] <http://www.fiz-karlsruhe.de>
- [13] <http://www.icdd.com>
- [14] M.I. Morozov, V. V. Gusarov, *Inorganic Materials* **38**, (7), 723–729 (2002).
- [15] M.I. Morozov, N.A. Lomanova, V.V. Gusarov, *Russian J. Gen. Chem.* **73** 1676 – 1680 (2003).
- [16] N.A. Lomanova, V. V. Gusarov, *Russian Journal of Inorganic Chemistry* **56**, (4), 616–620 (2011).
- [17] H.M.Rietveld, *Austr. J. Phys.* **41**, (2) 113-116 (1988).
- [18] A. Lisińska-Czekaj, D. Czekaj, *Archives of Metallurgy and Materials* **54**, (4) 870-874 (2009).
- [19] A. Lisińska - Czekaj, D. Czekaj, Z. Surowiak, J. Ilczuk, J. Plewa, A.V. Leyderman, E.S. Gagarina, A.T. Shuvaev, E.G. Fesenko, *Journal of the European Ceramic Society* **24**, 947–951 (2004).

